Schlussbericht, 9. Dezember 2005

Projekt Nr 47614

Direkte Numerische Simulation der Verbrennung bei höheren Reynoldszahlen

Autor und Koautoren	Dr. C. E. Frouzakis, Prof. Dr. K. Boulouchos
beauftragte Institution	Labor für Aerothermochemie und Verbrennungssysteme, ETHZ
Adresse	Sonneggstrasse 3, ETH-Zentrum, CH-8092, Zürich
Telefon, E-mail, Internetadresse	01 632 7947, frouzakis@lav.mavt.ethz.ch, www.lav.ethz.ch
BFE Projekt-/Vertrag-Nummer	47614/87714
Dauer des Projekts (von – bis)	1.10.2002-30.9.2005

ZUSAMMENFASSUNG

Direkte numerische Simulation kann sehr detaillierte und genaue Resultate in grosser räumlicher und zeitlicher Auflösung liefern, welche auf andere Weise nur schwer erhalten werden können. Diese Genauigkeit muss allerdings mit einem grossen Rechenaufwand bezahlt werden, welcher die Anwendung von effizienten numerischen Algorithmen und Parallelisierung für Simulationen von Strömungen mit hohen Reynoldszahlen unabdingbar macht. Während einem grossen Teil der Projektdauer wurden unsere Simulationswerkzeugen verbessert und den ausgebaut. Die Algorithmen unseres alten seriellen 2-D/axialsymmetrischen Codes wurden in einen parallelen 3-D Code für nicht reaktive Strömungen implementiert, welcher effiziente Lösungsverfahren verwendet und dessen Rechenleistung auf verschiedenen parallelen Systemen sehr gut mit der Anzahl verwendeter Prozessoren skaliert. Simulationen mit detaillierter Chemie und detaillierten Transporteigenschaften wurden durch die Verknüpfung mit den Chemkin Bibliotheken ermöglicht, und ein paralleler Integrator für steife Systeme wurde für die effiziente, implizite Integration der Spezies- und Energieerhaltungsgleichungen in den Code integriert. Dieser parallele Code wird für die Untersuchung von Strömungen in frühen turbulenten Bereich verwendet werden und dient als Basis für die Erweiterungen zur Grobstruktursimulation (Large Eddy Simulation) mit welcher turbulente Flammen modelliert werden können.

Was die Anwendungen anbelangt, wurden die Untersuchungen von Verbrennungsinstabilitäten weitergeführt, welche stark von einer Vielzahl von Parametern abhängen und für deren Erklärung und Verständnis eine Kombination von experimentellen und numerischen Resultaten nötig ist. Die seriellen und parallelen Codes wurden für die Simulation der transienten Veränderungen der Flammcharakteristik (Diffusions-/Edgeflamme) in Gegenstrahlbrennern, als auch für die Simulation von zellularen oder pulsierenden Flamminstabilitäten in Jet-Diffusionsflammen nahe der Auslöschung, eingesetzt. Zusätzlich werden momentan mit dem parallelen Code Simulationen der Interaktion von vorgemischten Flammen unterschiedlicher Dicke mit Turbulenz von unterschiedlicher Intensität und charakteristischer Wirbelgrösse durchgeführt. Die so generierten Resultate werden in die Entwicklung von Modellen für turbulente Verbrennung einfliessen.

BFE OFEN UFE SFOE

1 Project description

Direct Numerical Simulation (DNS) provides detailed information with high spatial and temporal accuracy that cannot be easily obtained by other means. The in-depth understanding of the physico-chemical processes of combustion phenomena that can be provided by the analysis of DNS results can also be used to validate or better understand the limitations of models currently available and guide their improvement.

Unfortunately, DNS carries a high computational cost and efficient numerical algorithms and parallelization are essential for the simulation of complex phenomena or problems at higher Reynolds numbers. A significant period of project time was invested in further enhancing and extending our computational capabilities. The algorithms of the serial 2-D and axisymmetric code were implemented in a parallel, non-reactive, three-dimensional code with efficient solvers and excellent scalability on a number of parallel architectures. The detailed description chemistry and transport were added by coupling the code with the Chemkin library, and the parallel stiff integrator PVODE was implemented for the more efficient, fully implicit integration of the species and energy conservation equations.

During the period of this project, our spectral element based DNS codes were used to study phenomena of fundamental interest in combustion. In order to understand the phenomena observed in experiments performed at the Paul Scherrer Institute, we used our axisymmetric serial code with detailed chemistry and transport to simulate diffusion/edge flames transitions (related to local extinction and re-ignition of turbulent diffusion flames) in opposed-jet geometries. The simulations showed that there is a complex interaction of the flow with the flame leading to unexpected flame dynamics.

The parallel code was used to study instabilities of jet diffusion flames close to extinction leading to either cellular flame formation (when the reactant Lewis number is less than unity), or pulsating flames (for reactant Lewis numbers higher than unity). Diffusion flame instabilities depend critically on a large number of parameters (initial mixture strength, Lewis numbers, proximity to extinction, fuel and oxidizer velocities). Consequently, both experimental and numerical information are required to elucidate the underlying physics. Single-step chemistry was used in these simulations, but detailed chemistry and transport were implemented and the code was coupled to a parallel stiff integrator for the efficient integration of the species and energy conservation equations.

The parallel code will be the main tool for the study of laminar and early turbulent combustion processes. In this context, we recently started work for the simulation of premixed flame/turbulence interactions. The code also forms the basis for the implementation of Large Eddy Simulation (LES) approaches for the simulation of turbulent combustion in practical devices.

2 Main results

2.1 Code development

Our simulation tools are based on the spectral element discretization of the partial differential equations describing the conservation equation of mass, momentum, species, and energy for chemically reactive systems at the low Mach number limit. The spectral element method combines the flexibility of the finite element method to discretize complex geometries with the high accuracy of spectral methods. Locally, the mesh is structured, with the data and geometry expressed as sums of N^{th}-order tensor product polynomials [4]. Globally, the mesh is an unstructured array of deformed hexahedral elements. Temporal discretization is based on a high-order, operator-splitting formulation for low speed compressible reacting flows that permits large time steps. More information about the numerical algorithm can be found in [1, 2, 3, 4].

In collaboration with Dr. Paul Fischer from the Argonne National Laboratories, we implemented the algorithms for reactive flow species and energy equations in his parallel, non-reactive, three dimensional, spectral element based code. This powerful code uses scalable domain-decomposition-based iterative solvers with efficient preconditioners. The parallel implementation is based on the standard message-passing Single Program Multiple Data (SPMD) mode, where contiguous groups of elements are distributed to processors and the computation proceeds in a loosely synchronous manner; communication is based on the MPI standard. The non-reactive code exhibits very good parallel efficiency and scalability properties, sustaining high MFLOPS, on a number of distributed-memory platforms. To take advantage of the reduction in problem size offered by axisymmetric geometries, the axisymmetric form of the conservation equations was also implemented and validated.

In the framework of a SNSF co-funded project, detailed chemistry and transport properties were added by coupling the code with the Chemkin package, and a parallel stiff integrator for the more efficient integration of the stiff differential equations. The general-purpose PVODE [5] integrator was implemented and validated against already available results. This development will allow us to perform DNS of combustion phenomena in the laminar and the early turbulent regime.

Turbulent reactive flows will be addressed with Large Eddy Simulations (LES). In another project funded by BfE, the code was used as the basis for the implementation of the Approximate Deconvolution Method (ADM) for LES [6]. Turbulent combustion will be modelled by flamelet and Conditional Moment Closure approaches.

2.2 Applications

2.2.1 Diffusion/edge flame transitions

Edge flames can appear under different conditions in premixed as well as non-premixed flames. In the latter case, edge flames can be observed at the lifted edge of laminar and turbulent jet flames, around the quenched region of a strained wrinkled flame in a turbulent flow, or a flat laminar flame, in flames spreading over a solid or liquid fuel, etc. In a turbulent diffusion flame, the local variation of the flow field can result in local extinction and the appearance of edge flames at the edges of holes in the diffusion flame sheet that can grow (leading to total flame extinction), shrink (flame re-ignition), or remain stationary.

Steady and transient edge flame phenomena in a two-dimensional axisymmetric opposed-jet burner were investigated with our serial DNS code using detailed chemistry and transport [7, 8, 9]. Cold walls were used to constrain the flow between the two nozzles and provide well-defined boundary conditions. Due to the high computational cost only the mixture of 40% H_2 in N_2 was considered, and the fuel and oxidizer velocities were varied, while constrained to be equal to each other. The range of flow rates over which the diffusion and edge flames are stable (stability limits) was numerically determined, showing the co-existence of the two flame types over an extended range and the associated hysteretic transition between the two flame types. The stabilization [8] and propagation characteristics [9] were studied in detail. In order to efficiently study the effect of fuel type, dilution, flow rate and burner geometry on the stability of counterflow edge and diffusion flames, a similar burner was constructed for experimental investigations at the Paul Scherrer Institute. Experiments with hydrogen and methane were carried out in different burners and with different dilutions. Chemiluminescence in the visible and ultraviolet (UV) and OH planar Laser-Induced Fluorescence (PLIF) were used in the first experiments to construct flame stability diagrams (velocity limits within which diffusion or edge flames can be stabilized). It was found that for fuel velocities greater than a specific critical value, crossing the boundary between edge and diffusion flame stability regimes leads to flame extinction. This was not expected, since the measured stability diagram suggested that instead a transition to a stable diffusion flame should have been induced. For a fuel consisting of 50% H_2 (by volume) in nitrogen, the flame structure was investigated in more detail experimentally by OH PLIF and 1-D Raman spectroscopy techniques. New simulations were validated against the experimental measurements and was then used to investigate the edge/diffusion flame transitions at conditions carefully selected from the experimentally determined stability diagrams in order to explain the unexpected flame dynamics.

Figure 1 shows the experimentally determined range of fuel and air velocities over which the diffusion and edge flames can be stabilized in the burner [10]. The diffusion flame was found to be stable in the region between the lines marked

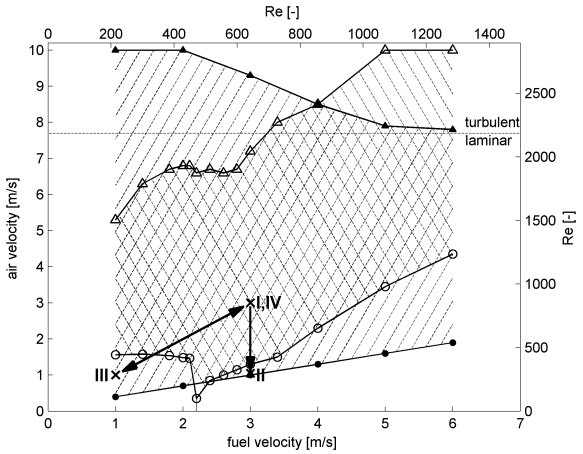

Figure 1: Stability diagram (velocity limits) for diffusion and edge flames for 50% H_2 in N_2 fuel composition. The diffusion flame is stable for flow velocities in the region delimited by filled symbols, and the edge flame in the region delimited by open symbols (d=5 mm tube diameter).

with open symbols, while the edge flame was stable in the range of flow velocities marked by the filled-symbol lines. In the cross-hatched region, both flames are stable and a transition from one flame type to the other could be induced by perturbing the flow field.

For $u_f = u_{air} = 3$ m/s both a diffusion and an edge flame can be stabilized. Figure 2 shows a comparison of the results from Raman scattering (left column) with the DNS (right column) for the edge flame obtained for $u_f = u_{air} = 3$ m/s. The concentrations of the major species O_2, H_2 and H_2O are shown; the axes are scaled by the burner tube diameter d=5.0 mm. The experimentally accessible range was 0.2 <z< 0.8 and 0 <r< 2.4 with a resolution of 0.1 on the z axis (step size of the burner translation) and of 0.02 in the radial direction (camera resolution).

The results for the O_2 concentration show that measurements and simulations are in good agreement in the region r >0.5, beyond the nozzle radius. Near the symmetry axis, however, the simulation predicts that O_2 is consumed closer to the air (upper) nozzle. The difference is more obvious for the H_2 mole fraction: in the simulation H_2 and O_2 impinge at $z \approx 0.3$, while from the measurements it must be concluded that they meet within the first mm above the lower disk. Cold-flow velocity measurements [10] in a similar burner configuration with disks attached have shown that the flow field itself possesses multiple asymmetric steady states, with the stagnation plane closer to either the upper or the lower nozzle. In the present case, the stagnation plane is close to the lower disk. With the stagnation plane so close to the jet exits, it is very likely that the imposed boundary conditions have a strong effect on the results, and the numerical domain needs to be extended into the nozzles for a more accurate prediction of the flow field.

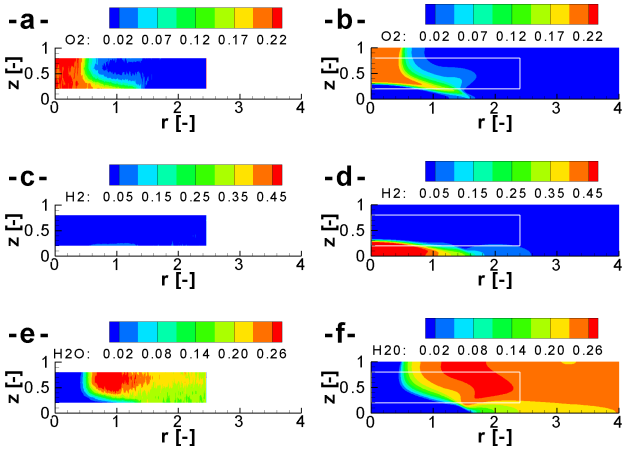

Figure 2: Experimental (left) and numerical (right) major species mole fractions in the edge flame ($u_f = u_{air} = 3m/s$): (a)-(b) oxygen, (c)-(d) hydrogen, (e)-(f) water. The figure axes are scaled with the burner tube diameter.

Figure 3 shows the temperature and OH distributions in the same flame. The predicted temperature distribution agrees very well with the experimentally determined one. Compared with the simulation, the measured OH profile is shifted by about 0.1 towards the symmetry axis and the air nozzle.

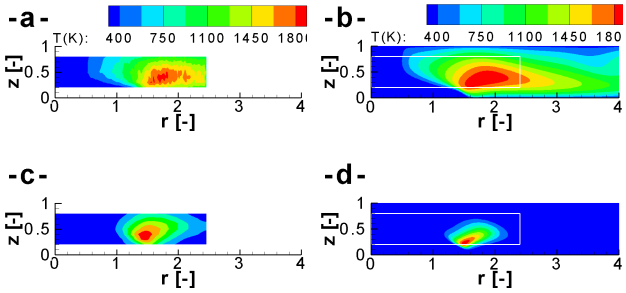

Figure 3: Experimental (left) and numerical (right) temperature (a-b) and OH (c-d) distribution in the edge flame.

For the same flow conditions a diffusion flame can also be stabilized. The comparison of the experimental and simulated results, shows that the same observations hold as for the edge flame above.

The lower stability limit of the edge flame of Fig. 1 (open circles) shows a characteristic inflection point (relative minimum) for u_f=2.15 m/s for the fuel mixture considered here. It was found that for u_f <2.15 m/s, a transition from an edge to a diffusion flame and vice versa is possible by suitably lowering/raising the air flow velocity, i.e. the flame shapes "switch" upon crossing the respective lower and upper stability limit. This behavior was predicted and analyzed in

detail in the numerical simulations of [9]. For fuel velocities to the right of this minimum, however, it was found experimentally that the edge flame extinguishes upon crossing its lower stability limit, even though a stable diffusion flame is possible there, as evidenced by the limit curve (filled circles). Similar behavior was found for other fuels, specifically 40% H_2 in N_2 as well as pure and diluted CH_4, using tubes with $d = 10$ mm and $d = 2.7$ mm diameter [10].

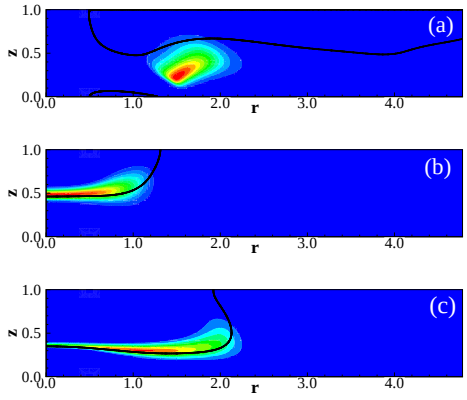

Figure 4: Simulation isocontours of the mass fraction Y_{OH} for (a) the edge flame for $u_f = u_{air}$ =3 m/s, (b) the diffusion flame for $u_f = u_{air} = 1$m/s, (c) the diffusion flame for $u_f = u_{air} = 3$m/s (bottom).

In order to understand the observed dynamics, additional numerical simulations were performed for conditions selected from the stability diagram. In the first simulation, starting from a previously-computed edge flame at other conditions, the conservation equations were integrated until the steady edge flame was established for $u_f = u_{air} = 3$ m/s (Fig. 4(a)). The flow field features two recirculation zones (a small one close to the lower fuel nozzle and a large one close to the air nozzle, marked by the black lines), which redirect the flow of the reactants through the flame. Taking this stationary solution as starting point, the second simulation was performed after impulsively reducing the air velocity to $u_{air} = 1$ m/s, while keeping u_f constant. These flow parameters correspond to a region in Fig. 1 where a stable diffusion flame can exist. Instead, the flame extinguishes, in agreement with the experimental observations. The analysis of the numerical results revealed the reason for the observed extinction: The decrease of the air velocity resulted in a sudden shift of the stagnation plane away from the fuel nozzle side, which then stabilized close to the air nozzle. The flame front did not propagate fast enough to follow the rather complicated fuel flow, and continued for a short time to burn closer to the fuel side. As it was deprived of oxygen, it could only be sustained until the oxygen remaining around it was consumed, leading to flame extinction. Starting from the same initial condition, a similar simulation was performed for $u_f = 1$ m/s, $u_{air} = 3$ m/s. No sudden jump of the

stagnation plane was observed in this case. The edge flame was squeezed close to the lower wall, where it continued to burn despite the significant drop in the maximum temperature due to the proximity to the cold wall.

In the final simulation, the starting point was again the stationary edge flame solution of the first run. Both air and fuel velocity were impulsively decreased to 1 m/s, i.e. to a region of Fig. 1 which is (a) to the left of the above-mentioned minimum, and where (b) only a diffusion flame can be stable. Indeed, such a stable diffusion flame was obtained (Fig. 4(b)) that is located slightly to the air side of the stoichiometric mixture fraction isoline (black line). This shows that it is not the flow velocity change *per se* which is responsible for the flame extinction found in the previous case. Rather, it is the rearrangement of the flow field associated with the sudden jump of the stagnation plane, for fuel velocities to the right of the inflection point, that leads to extinction.

Starting with this diffusion flame as an initial condition, in the final simulation fuel and air velocities were again increased to $u_f = u_{air} = 3$ m/s, thus bringing the flow parameters back to the starting point of the first (edge flame) simulation. A visibly strained, but stable diffusion flame resulted (Fig. 4(c)) around the stoichiometric mixture fraction isoline (black line), with markedly lower temperatures on the axis.

More details can be found in the paper attached to this report that has been submitted to the 31^{st} Combustion Symposium.

2.2.2 Cellular jet diffusion flames

The parallel code was used to simulate for the first time cellular diffusion flames. These have been observed experimentally at EPFL for jet diffusion flames close to extinction when the reactant Lewis number is sufficiently lower than one. The results were presented in the 30^{th} Combustion Symposium and were published in the Proceedings of the Combustion Institute.

The EPLF free jet apparatus, consists of a contoured axisymmetric contraction with an area ratio of 100:1. The circular fuel nozzle of diameter $D = 0.75$ cm is surrounded by a a porous plate of 7.5 cm diameter, where the oxidizer mixture is introduced. A systematic experimental investigation of cell formation in CO_2-diluted H_2-O_2 circular jet non-premixed flames was performed on this burner and the observed cellular flames can be seen in figure 5.

Three-dimensional simulations of the experimental setup were performed using single-step chemistry $2H_2 + O_2 \rightarrow H_2$, with reaction rate

$$r = A\, T^n\, \exp(-T_a/T)\, [H_2]^2\, [O_2]$$

and rate parameters $n = 0.91$, T_a=27.7 , and dimensionless heat of reaction ΔH_r=44.12. Constant but unequal Lewis numbers were used. Two resolutions were employed with 1166 and 2376 spectral elements with interpolating polynomial orders $6 \leq N \leq 8$ and $N = 4$ in each of the three spatial directions,

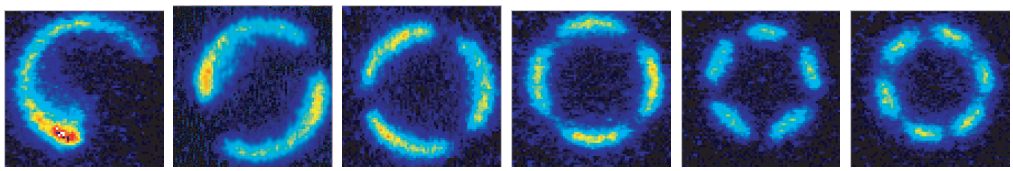

(a) 1R-cell (b) 2R-cell (c) 3R-cell (d) 4S-cell (e) 5S-cell (f) 6S-cell

Figure 5: Streamwise integrated chemiluminescence images of CO_2-diluted H_2 and in CO_2-diluted O_2 coflow jet flames. Images are taken downstream from the jet axis. "R" designates rotating and "S" stationary cell patterns.

respectively. The largest simulation had a total of about 600,000 points, corresponding to more than five million unknowns. By varying the dimensionless pre-exponential factor, A, the simulations captured the experimentally observed phenomena: existence of cellular structures with different number of cells close to extinction, co-existence of different cellular structures close to extinction (fig. 6), and sensitivity to noise, which can result in transitions from one cellular structure to another. More details can be found in the attached paper that appeared in the Proceedings of the Combustion Institute.

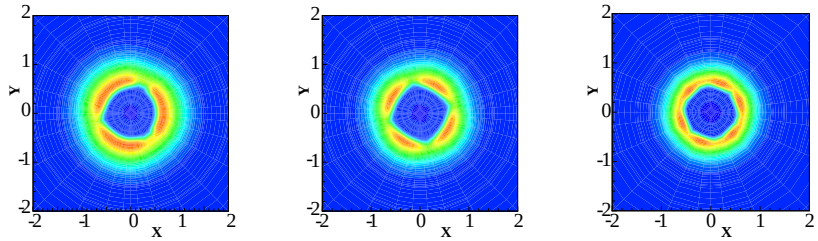

(a) (b) (c)

Figure 6: Temperature iso-contours of the (a) 3- ($A = 1.8 \cdot 10^8$, at z=0.8*D), (b) 4- ($A = 1.8 \cdot 10^8$, at z=0.8*D), and (c) 6-cell flame ($A = 2.5 \cdot 10^8$, at z=0.5*D)

2.2.3 Pulsating jet diffusion flames

Axisymmetric pulsating instabilities were also observed at the EPFL jet burner when the fuel Lewis number is larger than one, but the mechanism responsible for the onset and for driving them is not clear. The experimental setups was simulated with DNS using single-step chemistry and detailed transport. The fuel jet contained a propane mole fraction $X_{C_3H_8} = 0.122$ in nitrogen or a mass fraction $Y_{C_3H_8} = 0.1795$, and the centerline fuel velocity U_F was maintained at 25 cm/s, corresponding to a diameter-based Reynolds number of the fuel stream $Re = 144$, while the co-flowing oxidizer stream was maintained at $U_O = 5$ cm/s.

Thus, the velocity ratio of the coflowing streams, defined as R = (U_F - U_O) / (U_F + U_O) is equal to 0.667. In free shear flows, absolute instability, associated with the temporal amplification of disturbances superimposed on a base (parallel) flow is only present for sufficient back flow, i.e. velocity ratio values clearly higher than 1.0. The base flows are otherwise convectively unstable. Thus, the velocity and density ratio values of the present investigation suggest that global flow instabilities are not of a hydrodynamic origin.

The axisymmetric computational domain has a diameter equal to ten times the internal jet diameter, D, and height equal to $20D$. The fuel stream was N_2-diluted C_3H_8 with $Y_{C_3H_8} = 0.1795$ enters the domain at T=300K with the previously described velocity profile with a centerline velocity $U_F = 25$ cm/s, and the nozzle thickness is $\delta r_j = D/6$. The oxidizer is a O_2-N_2 mixture, entering at T=300K with the fitted profile specified above and $U_O = 5$ cm/s. The nozzle wall is also assumed to have a constant temperature of 300K. As in the experiments, the extinction limit was determined by starting the experiment with a stable, strongly burning flame and gradually decreasing the oxygen concentration in the oxidizer stream until, first, oscillations appeared, and then extinction was reached.

For the reactant species, flux (mixed) boundary conditions (BC) were used at the inflow, and zero-Neumann BC on the rest of the domain boundaries. On the lateral boundary, the slip wall BC with an axial velocity equal to U_O and fixed temperature BC was used. On the outflow boundary, zero normal stress BC were used for the momentum equation, and zero-Neumann BC for the rest of the variables. The mixture-averaged transport properties are calculated with the Chemkin routines. The reference variables used for non-dimensionalization are based on the properties of the fuel stream ($T_{\text{ref}} = T_F = 300$K, $U_{\text{ref}} = U_F$, and $t_{\text{ref}} = D/U_F = 0.03$ s). Chemistry was described by a single-step reaction, $C_3H_8 + 5O_2 \rightarrow 3CO_2 + 4H_2O$, with a non-dimensional reaction rate expression $RR = A\ \exp(-T_a/T)\ [C_3H_8]\ [O_2]$. The dimensionless reaction rate parameters were taken as $A = 4 \cdot 10^9$ and $T_a = 67.44$, and the heat of reaction was equal to $\Delta H_r = 203$. Gravitational effects were taken into account, but volumetric heat losses in the form of radiation were ignored.

The computational grid contained 988 spectral elements and interpolating polynomial orders equal to eight were used in each of the spatial directions. In all the simulations, the flame was contained within the high-resolution area. The computations were performed on 16 nodes of the Linux cluster at our Laboratory, and were continued for enough time to ensure either steady state or at least a few periods of saturated amplitude.

After allowing the fuel and oxidizer to mix, a hot source was added and the ignition process was computed which resulted in a burner-stabilized flame. As in the experiments, the oxygen concentration in the oxidizer stream was then reduced to bring the system close to extinction. The flame base first detached from the jet rim and stabilized at a certain lift-off height above the nozzle. The

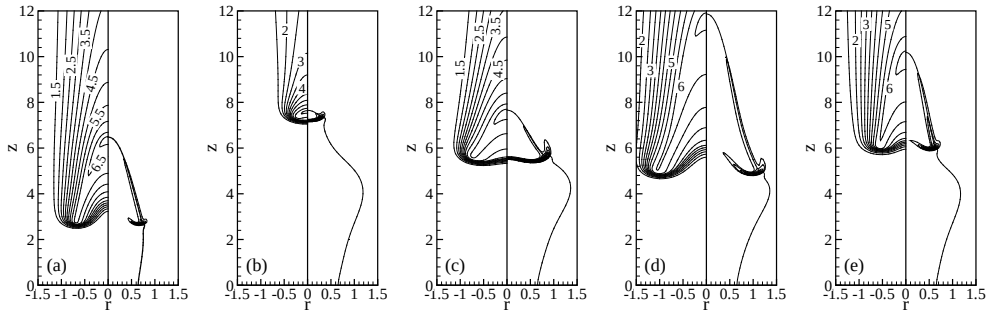

Figure 7: Isocontours of temperature (normalized by the fuel temperature, $T_f = 300K$ left half) and reaction rate (normalized by $\rho_F c_p T_F$, right half) of (a) steady lifted flame ($Y^0_{O_2}$=0.2280), and (b)-(e) the four time instants during one period of the pulsating flame for $Y^0_{O_2}$=0.205 marked by A, B, C, D in Fig. 8(e). The thick black line shows the stoichiometric mixture fraction isoline.

reaction rate isocontours (Fig. 7(a)) show the characteristic triple flame structure that is responsible for the stabilization, with a weak lean-premixed branch and a long diffusion tail along the stoichiometric mixture fraction isoline (indicated in the figure by the thick black line). When $Y^0_{O_2}$ was reduced to 0.228 the steady lifted flame first receded, and, instead of stabilizing further away from the nozzle, the flame edge reversed direction and propagated upstream, while the diffusion flame tail moved downstream, resulting in an increase of the flame length.

Fig. 8(a) shows the time history for both the integrated heat release rate HRR (solid line) and the maximum temperature T_{max} (dashed line). The peak-to-peak amplitudes of these signals decreased as the flame approached steady-state, and T_{max} also oscillated in phase with the HRR.

When the oxygen mass fraction in the co-flow was reduced to $Y^0_{O_2}$=0.2175, the HRR initially remained unaffected, and then dropped (see Fig. 8(b)) as the lower oxygen conditions in the slower co-flowing stream reached the flame-edge region, whereas the flame base moved farther downstream. As in the previous case, after some time, both the base and the tip of the flame started oscillating out of phase along the stoichiometric mixture fraction isoline. In this case, however, the relatively low amplitude pulsations did not die out and a sustained periodic contraction and expansion of the flame length along the stoichiometric mixture fraction Z_{st} isoline was observed.

As shown in Fig. 8(c), sustained pulsations of monotonically increasing amplitude were found down to $Y^0_{O_2}$=0.205. The edge flame was observed to oscillate or move between $4.83 \leq z/D \leq 7.25$, while the diffusion flame tail covered a wider range $7.13 \leq z/D \leq 12.88$. For $Y^0_{O_2} = 0.205$, Fig. 7(b-e) shows the reaction rate isocontours at the four points over a full pulsation period indicated by the letters A-D in Fig. 8(e). When the co-flowing oxygen concentration was reduced

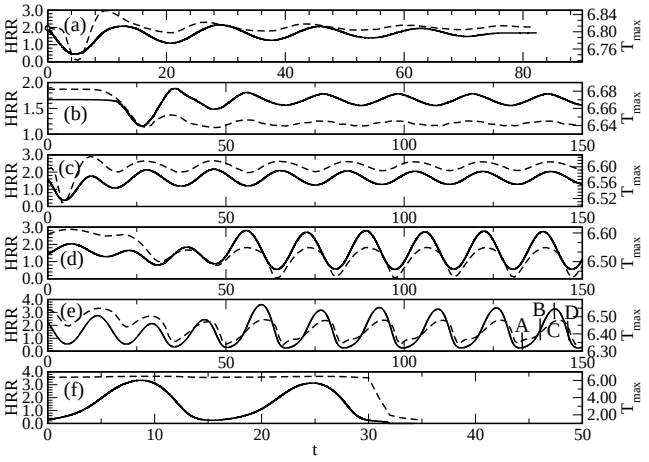

Figure 8: Time history of the normalized heat release rate (solid line) and maximum temperature (dashed line): (a) $Y^0_{O_2}$=0.2280, (b) $Y^0_{O_2}$=0.2175, (c) $Y^0_{O_2}$=0.215, (d) $Y^0_{O_2}$=0.21, (e) $Y^0_{O_2}$=0.205, (f) $Y^0_{O_2}$=0.2. Reference quantities as in figure 7.

further to $Y^0_{O_2} = 0.2$, after a couple of violent pulsations, the flame length reduced essentially to zero, due to the 180^o phase difference in the vertical movement of the flame base and flame tip and the flame extinguished (Fig. 8(d)).

Good agreement with the experiments was obtained in terms of pulsation frequency and the range of oxygen mass fraction in the oxidizer stream, $Y^0_{O_2}$, over which pulsations are observed. As also predicted by simple theoretical models that ignore hydrodynamic and detailed transport effects, pulsating flames appear in a narrow range of Da (a rescaled expression of $Y^0_{O_2}$) close to extinction, and the pulsation amplitude grows fast with decreasing of $Y^0_{O_2}$ (i.e. as the extinction is approached), eventually leading to the dynamic extinction of the flame when the pulsation amplitude becomes too large. The transition to the pulsating mode seems to be due to a super-critical Hopf bifurcation. However, very close to the critical point we have found multiple solutions (both steady and oscillatory states) for $Y^0_{O_2} = 0.218$, suggesting a narrow-range subcritical Hopf bifurcation. We are currently investigating the range of $Y^0_{O_2}$ values defining the hysteresis regime. The effect of gravity on the onset of the pulsations is analyzed with DNS in the absence of gravity.

More details can be found in the paper attached to this report that has been submitted to the 31^{st} Combustion Symposium.

2.2.4 Premixed flame/turbulence interactions

We have recently started the DNS of the interaction of an initially planar premixed flame with turbulence. The aim is to simulate the effect of turbulence with different intensities and characteristic length scales on premixed flames of

different thicknesses in order to obtain data for the development of new turbulent combustion models within the probability density function modelling approach. Model development will be performed in the group of Prof. Patrick Jenny of the Institute of Fluid Mechanics at ETHZ, within an ETH-funded project. First results can be seen in fig. 9. The synthetic homogeneous isotropic turbulence field was generated with the random field method of [11] and the initially planar premixed flame was computed with the code PREMIX from the Chemkin package using the single-step reaction $CH_4 + 2O_2 \rightarrow CO_2 + H_2O$ with rate constant $r = 1.92\ 10^{12} \exp(-15000/RT)[CH_4][O_2]$, resulting in a laminar flame speed of $S_L = 36$ cm/s for the stoichiometric methane/air mixture used.

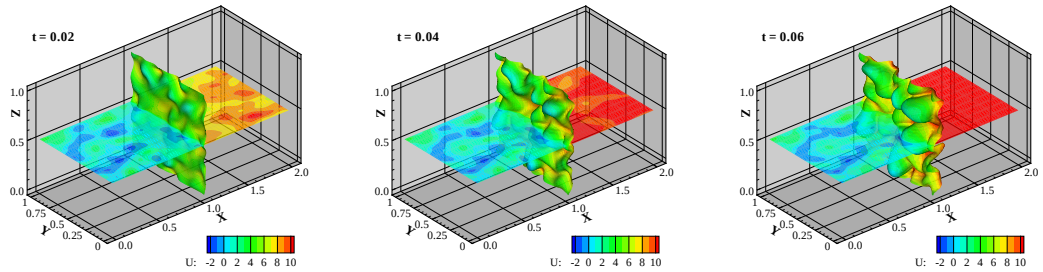

(a) (b) (c)

Figure 9: Vertical plane: T=1500K isosurface colored by the value of the non-dimensional x-component of velocity, U/S_L; horizontal plane: U isocontours at different non-dimensional times (a) t=0.02, (b) t=0.04, (c) t=0.06.

3 National collaborations

Diffusion/edge flame transitions are studied in a joint experimental/simulation effort. The experiments are performed at the PSI by Andrea Ciani and Wolfgang Kreutner in the combustion diagnostics group.

In collaboration with the Fluid Mechanics Laboratory of EPFL (group of Prof. P. Monkewitz), we are studying diffusion flame instabilities close to extinction. The work is a combination of experiments, numerical simulation and stability analysis.

Recently, we have started a collaboration with Prof. Patrick Jenny of the Institute of Fluid Mechanics at ETHZ. The aim is to perform direct numerical simulation of turbulent mixing under non-reactive and reactive conditions in order to obtain data for the development and validation of turbulent mixing models.

4 International collaborations

The parallel, three-dimensional reactive flow DNS code is being developed in collaboration with Dr. Paul Fischer of Argonne National Laboratory, USA.

In the framework of the simulation of diffusion flame instabilities, we are working together with Prof. Paul Papas of the Colorado School of Mines, Colorado, USA.

A joint effort with Prof. Ananias Tomboulides of the University of Western Macedonia, Kozani, Greece aims in the implementation of Large Eddy Simulation models in our code.

In a recently started project, bluff-body flame stabilization is investigated together with Prof. Lambros Kaiktsis from the Department of Naval Architecture and Marine Engineering, National Technical University of Athens, Greece.

5 Conclusions and outlook

In the course of this project, our computational tools were significantly expanded and enhanced. First, the algorithms for low Mach number reactive flows were implemented in a parallel, non-reactive, three dimensional, spectral element based code. This powerful code uses scalable domain-decomposition-based iterative solvers with efficient preconditioners and has shown excellent scalability in a number of parallel architectures. The full three dimensional as well as the axisymmetric form of the conservation equations were implemented and validated. Second, detailed chemistry and transport have been implemented and the code was coupled with the general-purpose parallel stiff integrator PVODE.

In terms of applications, the older serial code was used to interpret experimental observations during diffusion/edge flames transitions in the PSI counterflow burner. The linear scalability of the new reacting flow code enabled the first simulation of cellular jet diffusion flames in the full three-dimensional context. Axisymmetric jet diffusion flame pulsations close to extinction are also studied in detail in order to understand the processes that are responsible for initiating and sustaining the pulsations.

The tools developed will allow us to place emphasis in the simulation of reactive flows in the early turbulent regime. For example, we recently started direct numerical simulations of turbulent mixing under reactive and non-reactive conditions. The data will be used for the development of turbulent mixing and combustion models in the framework of probability density function methods. Higher Reynolds number flows will be studied with large eddy simulation models that are currently under development.

6 Publications

- C.E. Frouzakis, A.G. Tomboulides, P. Papas, P.F. Fischer, R.M. Rais, P. Monkewitz, and K. Boulouchos, "Three-dimensional numerical simulations of cellular jet diffusion flames", *Proc. Comb. Inst.*, **30**, (2005).

  A. Ciani, W. Kreutner, W. Hubschmid, C.E. Frouzakis, K. Boulouchos, "Experimental investigation of the structure and stability of planar and toroidal flames in an opposed jet burner", *submitted to Combust. Flame* (2005)

- C. E. Frouzakis, A. G. Tomboulides, Paul Papas, Lambros Kaiktsis, Konstantinos Boulouchos, "Numerical Simulations of Jet Diffusion Flame Pulsations Close to Extinction", *Proc. Comb. Inst.*, (submitted), (2005).

- A. Ciani, W. Kreutner, C. E. Frouzakis, K. Boulouchos, "Counterflow edge flames: their structure and dynamics at extinction limits", *Proc. Comb. Inst.*, (submitted), (2005).

The publications are appended at the end of the report.

References

[1] P.F. Fischer and H.M. Tufo, High-performance Spectral Element Algorithms and Implementations, in Parallel Computational Fluid Dynamics: towards Teraflops, Optimization and Novel Formulations, in D.Keyes, A. Ecer, N. Satofuka, P. Fox, and J. Periaux, (eds.) North-Holland, 17–26, (2000).

[2] A.G. Tomboulides, J. Lee, and S.A. Orszag, Numerical simulation of low Mach number reactive flows, *J. Sci. Comp.*, **12**(2) 139–167, (1997).

[3] A.G. Tomboulides, and S.A Orszag, A quasi two-dimensional benchmark problem for low Mach number compressible codes, *J. Comp. Phys.*, **146**(2), 691–706, (1998)

[4] M.O. Deville, P.F. Fischer, and E.H. Mund, *High-Order Methods for Incompressible Fluid Flow.* Cambridge University Press, (2002).

[5] G.D. Byrne, A.C. Hindmarsh, PVODE, an ODE Solver for Parallel Computers, Intl. J. High Performance Comp. Appl., **13**(4), 354-365, (1999)

[6] S. Stolz, N. A. Adams, An approximate deconvolution procedure for large-eddy simulation, *Phys. Fluids*, **11**(7), 1699-1701 (1999).

[7] J. Lee, C. E. Frouzakis, K. Boulouchos, "Opposed-Jet Hydrogen/Air Flames: Transition from a Diffusion to an Edge Flame", *Proc. Combust. Inst.* 28 (2000) 801–806.

[8] C. E. Frouzakis, A. G. Tomboulides, J. Lee, K. Boulouchos, "From diffusion to premixed flames in an H_2/air opposed-jet burner: the role of edge flames", *Combust. Flame* 130 (3) (2002), 171–184.

[9] C. E. Frouzakis, A. G. Tomboulides, J. Lee, K. Boulouchos, "Transient phenomena during diffusion/edge flame transitions in an opposed-jet hydrogen/air burner", *Proc. Combust. Inst.* 29 (2003) 1581–1587.

[10] A. Ciani, W. Kreutner, W. Hubschmid, C.E. Frouzakis, K. Boulouchos, "Experimental investigation of the structure and stability of planar and toroidal flames in an opposed jet burner", *submitted to Combust. Flame* (2005)

[11] A. Smirnov, S. Shi, I. Celik, Random flow generation technique for large eddy simulations and particle-dynamics modeling *ASME: J. Fluids Eng.*, **123**(2), 359-371, (2001).